siRNA associated with immunonanoparticles directed against cd99 antigen improves gene expression inhibitionin vivoin Ewing's sarcoma

Anne-Laure L Ramon, J. R Bertrand, H. de Martimprey, G. Bernard, G. Ponchel, C. Malvy, Christine Vauthier

SiRNA associated with immunonanoparticles directed against cd99 antigen improve gene expression inhibition *in vivo* in Ewing's sarcoma.

Ramon AL[a,b,c,d], Bertrand JR [a,d] , de Martimprey H [a,b], Bernard G[d], Ponchel, G [b,c] Malvy C [a,e], Vauthier C [b,c]

a CNRS UMR 8203 Vectorologie et thérapeutiques anticancéreuses, 114 rue Edouard Vaillant, 94805 Villejuif Cedex, France
b Univ Paris-Sud, Faculté de Pharmacie, 5 Rue J.B. Clément, F 92296 Châtenay-Malabry France
c CNRS UMR 8612, Institut Galien Paris-Sud, 5 Rue J.B. Clément, F 92296 Châtenay-Malabry France
d. INSERM U.3433, Nice, France
e Univ Paris-Sud, F-94805 Villejuif, France

Running title: Immunonanoparticles targeting siRNA to treat Ewing's Sarcoma

Corresponding author : Christine Vauthier. Univ Paris Sud, Institut Galien Paris-Sud, Faculté de Pharmacie, 5 Rue J.B. Clément, F 92296 Châtenay-Malabry France
Email: Christine.vauthier@u-psud.fr, Phone: 33 1 46 83 56 03, Fax : 33 1 46 83 53 12

This work was published in : *J. Mol. Recognit. 2013; 26: 318–329. DOI: 10.1002/jmr.2276*

Abstract

Ewing sarcoma is a rare, mostly pediatric bone cancer which presents a chromosome abnormality, called EWS/Fli-1, responsible for the development of the tumours. *In vivo*, tumour growth can be inhibited specifically by delivering siRNA associated with nanoparticles. The aim of the work was to design targeted nanoparticles against the cell membrane glycoprotein cd99 which is over expressed in Ewing sarcoma cells in order to improve siRNA delivery to tumour cells. Biotinylated poly(isobutylcyanoacrylate) nanoparticles were conceived as a platform to design targeted nanoparticles with biotinylated ligands and using the biotin-streptavidin coupling method. The targeted nanoparticles were validated *in vivo* for targeted delivery of siRNA after systemic administration to mice bearing a tumor model of the Ewing sarcoma. The expression of the gene responsible of Ewing sarcoma was inhibited at 78 ± 6 % by associating the siRNA with the cd99 targeted nanoparticles compared with an inhibition of only 41 ± 9 % achieved with the non targeted nanoparticles.

Key words: Ewing sarcoma, siRNA, immunonanoparticles, poly(alkylcyanoacrylate) nanoparticles, chitosan

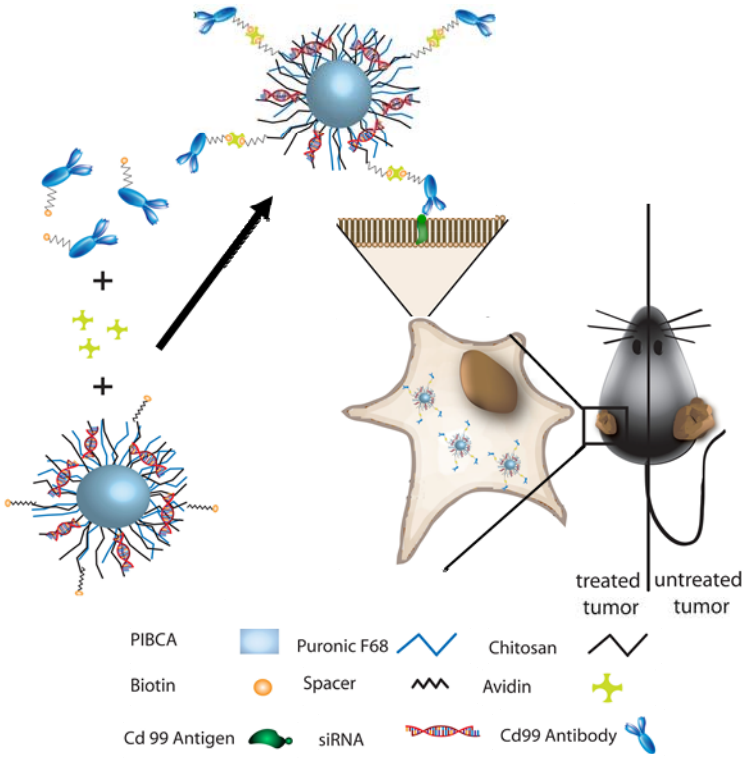

Introduction

Ewing's sarcoma is a rare, mostly pediatric, bone cancer affecting mostly children and young adults before 20 years old. It is a very aggressive disease with low survival rates, around 63% for localized disease and 32% for metastatic disease at 10 years [Esiashvili et al., 2008].

In 85% of the cases, it is associated with the t(11;22) (q24:q12) chromosomal translocation leading to the traduction of the EWS/Fli-1 fusion protein [Delattre et al., 1992, Turc-Carel et al., 1984] . This chromosomal abnormality is known to be responsible for Ewing's sarcoma features in various cell types [Hu-Lieskovan et al., 2005a, Rorie et al., 2004] and cell tumorigenicity in mice [May et al., 1997].

RNA interference (RNAi) mediated by small interfering RNAs (siRNAs) allows inhibiting a specific gene by targeting and degrading its mRNA sequence. Since their discovery in 2001, siRNAs have been studied as potential new therapeutic agent against cancer, including Ewing's sarcoma. Several siRNA sequences targeting the junction oncogene EWS/fli-1 have been studied and were shown active both *in vitro* and *in vivo* [Alhaddad et al. 2011, Hu-Lieskovan et al., 2005b, Takigami et al., 2011, Toub et al. 2006] . As all oligonucleotides, siRNA are poorly stable in biological fluids. It is necessary to protect them to achieve successful *in vivo* delivery. To this aim, one of the strategies currently used is carrying siRNA using nanoparticles to protect and distribute them in the blood stream down to their target. Main types of drug delivery systems that can be found in the literature for the delivery of siRNA are lipo and polyplexes, which are advantageously formed using the polyanionic nature of the siRNA. Among all suggested nanocarriers, successful *in vivo* delivery of siRNA was reported using a polymeric carrier made of poly(isobutylcyanoacrylate) (PIBCA)/chitosan core/corona nanoparticles [de Martimprey et al. 2008, 2009] . The choice of this type of nanoparticle was driven by several of their characteristic: Firstly, those nanoparticles have a cationic and hydrophilic shell; hence they are good candidates for the efficient complexation of hydrophilic polyanionic molecules such as siRNA. Secondly, the chitosan corona gives these nanoparticles stealth characteristics and thus a longer residence time in the blood stream. Finally, the size of these PIBCA/chitosan nanoparticles is under 100nm, which allows a good distribution of the nanoparticles in the body and possible distribution in tumor by an enhanced permeation and retention effect. Additionnally, the synthesis of these nanoparticles results from a scalable process while their small size makes them suitable for sterilization by filtration. Both characteristics are important for developing nanoparticles with industrial applications. Efficiency of those nanoparticles may further be enhanced by improving their capacity to address specifically the siRNA to the target cells, *i.e.,* the Ewing's sarcoma tumor cells. This would also reduce the siRNA doses needed for the treatment in human hence the cost and the possible adverse effects. Generally, nanoparticles can be targeted by various means, for example by addition of RGD motives which target the integrins or by grafting of transferrin, which receptor is over expressed in numerous tumors (a review on the use of targeted and untargeted drug delivery systems for siRNA can be found here [Daka and Peer 2012]). Targeting Ewing Sarcoma's tumors has already been successfully reported by Hu-Lieskovan *et al* [Hu-Lieskovan, Heidel, et al. 2005b] using transferrin. However, although very efficient, a more specific method of targeting could be the use of monoclonal antibodies targeting against a specific surface antigen expressed by the tumor. This was done previously on other models with other types of nanoparticles [Lin et al., 2012, Liu et al., 2012, Lv et al., 2012, Saxena et al., 2010, Srinivasan et al., 2012, Wang et al., 2012] but to our knowledge it wasn't reported in the case of Ewing's Sarcoma. In the present study, the targeting method is based

on the grafting of the anti-cd99 antibodies on the chitosan corona of the PIBCA nanoparticles. This antibody is specific to the cell surface cd99 which is a cell surface glycoprotein overexpressed in Ewing's sarcomas family tumor cells (ESFT) [Ambros et al., 1991, Dubois et al., 2010]. Attachment of the antibodies on the nanoparticle surface can be achieved according to a method based on the formation of an avidin-biotin complex suggested by Segura-Sanchez *et al*. [Segura-Sanchez et al. 2010]. This approach allows flexibility in the choice of ligands including antibodies to be grafted onto the surface of the nanoparticles in the future. Thus, the aim of the present work was to conceive immunonanoparticles using the chitosan decorated PIBCA nanoparticle drug delivery plateform and to evaluate their potential to improve *in vivo* delivery of siRNA in a human Ewing's sarcoma tumor xenografted to nude mice. Performance of the immunonanoparticles was compared with that of the non targeted nanoparticles.

1. Material and methods

1.1. Material

Pluronic® F68 (Lutrol F68) was provided by BASF (Germany). Chitosan middle-viscous was supplied by Fluka (Germany). Chitosan was hydrolyzed by the method previously used by Bertholon *et al.* [Bertholon et al., 2006] using 90mg of $NaNO_2$ for 2g of chitosan diluted in 100mL of acetic acid 6%. The molecular weight of chitosan chain was 20.2 kDa as determined by capillary viscosimetry.

EZ-Link® TFP-PEO_3-biotin, EZ-Link® Sulfo-NHS-LC-Biotin, EZ-link® Biotin-LC-hydrazide and EZ-link® Biotin-PEG_4-hydrazide were purchased from Pierce, Thermo Fisher Scientific, USA. IsoButylCyanoAcrylate (IBCA) was provided as a gift by Henkel Biomedical, Ireland. The siRNAs were purchased from Eurogentec (Brussels, Belgium). The sequence was chosen to be complementary to the EWS/Fli-1 fusion oncogene: sense strands: 5' GCAGCAGAACCCUUCUUAUd(GA) 3') and antisense strand : 3' d(CC)CGUCGUCUUGGGAAGAAUA 5'. The control sequence was sense strand: 5' – GCCAGUGUCACCGUCAAGGdAdG – 3' and the antisense strand: 5' – CCUUGACGGUGACACUGGC dTdT – 3'. The siRNAs were purchased from Eurogentec (Brussels, Belgium). Primers for RT-PCR experiment were purchased at Eurogentec (Belgium) with sequence: EWS -F 5'-AGC AGT TAC TCT CAG CAG AAC ACC-3'; Fli-1 -R 5'-CCA GGA TCT GAT ACG GAT CTG GCT G-3'; mcherry -R 5'TCA TCA CGC GCT CCA CTT GA-3'; mcherry-F "TCC GTG AAC GGC CAC GAG TT-3'.

Jurkat cells were provided by Pr. A. Bernard (INSERM U.3433, Nice, France). A673 and TC71 were human Ewing sarcoma cells and were a generous gift from Dr. Elizabeth R. Lawlor (University of Michigan, USA).

Specific antibodies to Ewing's Sarcoma were cd99 antibodies obtained from the laboratory of Pr. A. Bernard (INSERM U.3433, Nice, France). These antibodies were selected by Pr. A. Bernard for their absence of toxicity. Control antibodies with no specificity for Ewing sarcoma cells were purchased from BD Pharmingen as purified mouse IgG 2a k, isotype control (ref 555571).

1.2. Methods

1.2.1. Synthesis of PIBCA/Chitosan nanoparticles by Redox Radical Emulsion Polymerization

PIBCA/Chitosan nanoparticles were synthesized by redox radical emulsion polymerisation (RREP) according to de Martimprey *et al.* [de Martimprey et al., 2008]. The hydrolyzed chitosan (0,0688 g) and 3.5 % of Lutrol F68 were dissolved in an aqueous solution of nitric acid (4 mL, 0.2 N) in a glass bottle at 42°C under strong magnetic stirring and argon bubbling. After 10 min, a solution of Cerium (IV) ammonium nitrate (1 mL, 80 mM in 0.2 N nitric acid) was added. Immediately after, 250 µL of IBCA were added under vigorous stirring and argon bubbling was maintained for 10 min. The reaction was allowed to continue at 42°C for 50 min. After cooling in an ice bath for 5 min, the dispersion was dialyzed (Spectra/Por membranes, MWCO: 100,000, Biovalley) four times for 30 min, 30 min, 1h, 1h and overnight against 1L of MilliQ® water acidified with 1mL of acetic acid 16mM.

To label the core of the nanoparticles, 800µL of a rhodamine labelled monomer, PolyFluor® 570 (methacryloxyethylthiocarbamoyl rhodamine B (N-[9-(2-carboxy-x-methacryloxyethylthiolcarbamoyl-phenyl)-6-diethylamino-3H-xanthen-3-ylidene]-N-ethyl-ethanaminium chloride, Polyscience, BioValley, France) solution in acetonitrile (2 mg/mL) was added to the polymerization medium 2 min after the addition of the monomer [Bravo-Osuno et al., 2007] .

1.2.2. Preparation of the immunonanoparticles

PIBCA/Chitosan nanoparticles were first diluted to 10mg/mL in MilliQ® water. EZ-Link® TFP-PEO_3-biotin or EZ-Link® Sulfo-NHS-LC-Biotin were added at concentrations of 0.7 mmol/L and 1.4 mmol/L to the nanoparticle dispersion to achieve nanoparticle biotinylation and let to react on a rotating wheel at room temperature for 2 h in the dark. Samples were dialyzed against sterile water (Spectra/Por® membranes, MWCO: 100,000, Biovalley) for 30 min, 30 min, 1h, 1h and overnight to remove any excess of reactant.

For antibody biotinylation, antibodies were first oxidized using 250 nM sodium metaperiodate (Sigma-Aldrich, USA) in AcONa/AcOH 0.2 N, pH 5.5, 30 min, 4°C in the dark. After several washings with reaction buffer, oxidized antibodies were coupled to biotin using EZ-link® Biotin-LC-hydrazide or EZ-link® Biotin-PEG_4-hydrazide in various amounts.

To insure efficient coupling and avoid nanoparticle aggregation we chose to use a two step complex formation. First, biotinylated antibodies were associated with an excess of neutravidin (NeutrAvidin Protein, Pierce Thermo Fisher Scientific, USA), during 2 h. After three washings with desalting columns (100 k centrifugal filter units, Millipore, USA) in order to remove the unreacted neutravidin, antibodies diluted in 50 µL of MilliQ® water were mixed with 50 µL of nanoparticles (10 mg/mL) and left overnight on a rotating wheel for equilibration.

1.2.3. Nanoparticle Characterization

Particle Size: The hydrodynamic diameter of the PIBCA/Chitosan nanoparticles was determined at 25°C by quasi-elastic light scattering with a Zetasizer nano ZS90 (Malvern Instrument Ltd, France), operating at 90°. 20 µL of each sample was diluted in 1 mL of MilliQ® water. The temperature was allowed to equilibrate 5 min before measurement. Results show the mean hydrodynamic diameter of

the nanoparticles obtained from at least three measurements on three different preparations of nanoparticles.

***Zeta Potential*:** Zeta potential was measured using a Zetasizer nano ZS90 (Malvern Instrument Ltd, France). 80 µL of nanoparticle dispersion were diluted in 2 mL of NaCl 1 mM. The measurements were repeated at least three times on three different preparations of nanoparticles.

***Transmission electron microscopy*:** Transmission electron microscopy (TEM) was performed using a Philips EM208 with a large format CCD camera AMT at the CCME Orsay. The samples were diluted in MilliQ® water 1:100 and deposited on a carbon-coated formwar film on copper grids. After 5 min, the excess was removed and stained with neutral 1% aqueous phosphotungstic acid for 30 s.

***siRNA labelling and adsorption onto nanoparticles*:** siRNAs were labelled at 5' terminal end using T4 polynucleotide kinase (New England Biolabs) and [γ^{32}P] (6000 mCi/mol) as indicated by the supplier. After 1 h incubation at 37°C, labelled siRNAs were separated from unreacted material by gel filtration (Sephadex® G25 Column) and centrifugation (1500 rpm/min).

Various amounts of PIBCA/Chitosan nanoparticles and siRNA were dissolved in a final volume of 300 µL of water or HEPES buffer (10 mM HEPES pH 7.3, 100 mM NaCl) and briefly mixed. NP:siRNA or NP:siRNA mass ratios ranged from 1:0 to 1:300. After 10 min of incubation, nanoparticles were ultracentrifuged (45 000 rpm, 1 h). After centrifugation, radioactivity was measured in supernatants. Each experiment was repeated three times.

***Activation of the complement system*:** Activation of the complement system was evaluated using 2D immunoelectrophoresis as described previously [Bertholon, et al., 2006a, Bertholon et al., 2006b, Bravo-Osuna et al., 2007, Vauthier et al., 2011]. Briefly, the nanoparticles (400 cm^2 in 100 µL) were incubated with 50 µL of human serum and 50 µL Veronal buffer containing 0.15 mM calcium chloride and 0.5 mM magnesium chloride for 1 h at 37 °C. After incubation, 7 µL of each sample was migrated on a 1% agarose gel. Each strip of the first electrophoresis was migrated on Gelbond® films in 1% agarose gel plates with a human C3 polyclonal antibody (Goat complement C3 antiserum, Sigma, France), recognizing both C3 and C3b. The Gelbond® films were dried and stained with Coomassie blue to reveal the presence of C3 and C3b. The complement activation factor (CAF) was calculated from the ratio of the area of the peak attributed to C3b over the sum of the areas of the peaks attributed to C3b and to C3.

$$CAF = 100 \cdot \frac{\mathrm{C3b}}{\mathrm{C3b} + \mathrm{C3}}$$

1.2.4. Characterization of the functionality of the biotin grafted onto PIBCA/Chitosan nanoparticles and on the antibodies

Efficiency of the coupling reaction of the biotin spacer onto the PIBCA/Chitosan nanoparticles was determined using HABA/Avidin colorimetric reaction (HABA/Avidin reagent, Sigma-Aldrich, USA). The control sample was the unbiotinylated PIBCA/Chitosan nanoparticles.

To check the coupling efficiency of the biotin on the antibodies, we used flow cytometry with streptavidin-FITC (Streptavidin−FITC from *Streptomyces avidinii*, Sigma-Aldrich, USA) as a revelation agent or TEM using gold-avidin (Streptavidin−Gold from *Streptomyces avidinii*, Sigma-Aldrich, USA) as a revelation agent.

Flow cytometry was performed according to the following protocol: first, a suspension of cd99-expressing Jurkat cells at a concentration of 2.5 10^6 cells/mL was prepared. 200 µL of the cell suspension (5,100 cells) were plated in a 96-well plate, centrifuged and the pellets were rinsed twice with cold PBS buffer to remove the culture medium. After centrifugation at 4°C, cells were suspended in 20 µL of cold PBS buffer containing 0.5 µg of biotinylated anti-cd99 antibody and incubated on ice at 4°C during 1h. Cells were then rinsed twice with 200 µL of cold PBS buffer and centrifuged at 4°C. The resulting pellet was resuspended in 20 µL of cold PBS buffer containing 4µg of streptavidin-FITC as a revelation agent and incubated another hour in the dark on ice at 4°C. After 2 more washings with 200 µL ice cold PBS, samples were suspended in 200 µL of ice-cold PBS and analyzed using a flow cytometer (FACS Calibur, BD Biosciences, USA).

1.2.5. Characterization of the immunonanoparticles: Biotin-avidin specific recognition

To assess the efficiency of the coupling reaction of the antibodies through the specific biotin-avidin sandwich, we used both western blotting technique and bicinchroninic acid (BCA) dosage. BCA dosage was previously used as a technique to assess the amounts of antibodies grafted to PLGA nanoparticles by Nobs *et al.* [Nobs et al., 2003].

For both experiments, an aliquot of coupled nanoparticles was centrifuged and 10 µL of the supernatant was used for SDS-PAGE (Sodium Dodecyl Sulphate- Poly-Acrylamide Gel Electrophoresis) analysis or BCA testing.

For western blotting, samples were boiled at 95°C with Nu PAGE® sample Buffer 4x and Nu PAGE® reducing agent during 5 min. Then samples were loaded on precast 12% polyacrylamide gels (Pierce, Thermo Fisher Scientific, USA) and migrated at 200 volts for 50 min. The proteins were transferred on a nitrocellulose membrane using semi dry transfer for 1h30 at 25 V. The membrane was blocked in 5% nonfat milk in PBS-Tween (0.1%) for 1 h. Then the membrane was incubated overnight at 4°C with a goat anti-human antibody coupled to horseradish peroxidase (Jackson Immunoresearch, USA) diluted to 1/500. Proteins were visualized with an enhanced chemoluminescent (ECL) system (GE Healthcare, UK).

For BCA, 10 µL samples were mixed with 10 µL of reconstituted BCA reagent (Pierce BCA Assay kit, Pierce) and incubated for 1 h at 37°C in the dark. The optical density (OD) of each sample was measured at 562 nm using a 96-well plate reader as indicated by the manufacturer (MRX II & MRX Model 96 Well Plate Reader, Dynex). The concentration of the antibodies retrieved in the supernatant was determined by comparing the OD of the sample to a standard curve as advised by the manufacturer of the BCA dosage kit.

1.2.6. Evaluation of the cytotoxicity of the nanoparticles

For toxicity studies, A673 cells from a patient an Ewing's sarcoma tumor were cultivated in Dulbecco's Modified Eagle Medium (D-MEM) with glutamax (Gibco) containing 10% of heat-inactivated bovine foetal serum, penicillin (100U/mL) and streptomycin (100U/mL). Cultured cells

were regularly tested for the presence of mycoplasma with MycoAlert® Mycoplasma Detection Kit (Lonza, Basel, Switzerland). Cells were plated in 96-well plate at 104 cells per well and cultivated for 24 h at 37°C, 5% CO_2 and 95°C humidity. After 24 h, culture medium was removed and replaced by a dispersion of nanoparticles in culture medium, concentrations ranging from 0 to 1000 µg/mL. The cells were allowed to grow for 24 h. Then the culture medium was replaced by 100 µL of a solution of dimethylthiazol diphenyl tetrazolium bromide (MTT) solution (0.5 mg/mL in PBS) and incubated at 37°C for 3 h. After incubation, 100 µL of 10 mM hydrochloric acid/10% sodium dodecyl sulphate solution was added to each well and allowed to solubilise formazan crystals overnight. Each plate was read on a microplate reader (MRXII, Dynex Technology) at a wavelength of 570 nm. Untreated cells were used as control. Each nanoparticle concentration was evaluated three independent times, and each measurement was made in triplicate.

1.2.7. Characterization of the expression of the glycoprotein cd99 expression on the Ewing sarcoma cell lines

To assess cd99 expression in our laboratory cell lines, 5 10^5 Jurkat, A673 or TC71 cells were incubated with 0,5 µg of anti-cd99 antibody, 1 h, 4°C on ice in dark. After three PBS washing, cd99 recognition was revealed using a FITC-anti mouse antibody (0.5 µg) incubated for 1 h at 4°C on ice in the dark. Staining was revealed using flow cytometry (BD FACSCalibur, BDbiosciences, USA).

1.2.8. Efficient recognition of the cd99 membrane protein by the immunonanoparticles

For confocal microscopy, A673 cells were plated on cover glasses in 6-Well plates and allowed to grow for 24 h cultured in complete medium. After 24 h the culture medium was removed and replaced by OptiMEM for 30 min at 4°C on ice. Then OptiMEM was removed and replaced by OptiMEM containing Rhodamine labeled nanoparticles. The cells were incubated 30 min at 4°C on ice, then rinsed three times with cold PBS and fixed with cold paraformadehyde 4 %. Cover-glasses were mounted using 10 µL of Dapi-Fluoromount prior to the observation with a confocal microscope SPE Leica (Leica Microsystems GmbH, Germany) from the microscopy plateform of the Institut Gustave Roussy.

1.3. *In vivo* efficiency of the immunonanoparticles

All the animal experiments were performed under the French laws on animal experimentation and the protocols were approved by the ethic committee on animal experimentation of the Institut Gustave Roussy.

1.3.1. Tumor growth inhibition

Nude mice (env. 30 g weight) were injected subcutaneously in the left flank with A673 cells (2,5.10^6 cells/mouse). 50 mm^3 tumor-bearing nude mice (env. 30 g weight) were treated by intravenous injections (tail vein) of siRNA associated with PIBCA/Chitosan nanoparticles at two cumulated dose levels (7 mg/kg divided in five injections, each injection having a final volume of 100 µL/mouse). Tumor size was evaluated up to 24 days after the first day of treatment using an electronic caliper.

1.3.2. Measurement of the inhibition of EWS/Fli-1

Nude mice were injected subcutaneously in the left flank with A673 cells (2,5.10^6 cells/mouse). Tumor-bearing nude mice (env. 30 g weight) were treated by intravenous injections of siRNA

associated or not with the PIBCA/Chitosan nanoparticles or with the immunonanoparticles. All the nanoparticles used were dispersed in a 0.9% saline solution. The total cumulative dose of siRNA injected was 120 µg/kg divided in 5 injections of 24 µg/kg diluted in a volume of 100 µL per injection. Control experiments were performed using physiological serum (0.9% saline solution), as well as free siRNA at the same dose (120 µg/kg cumulative dose) or empty nanoparticles dispersed in physiological serum at concentrations used in the experiments performed with the siRNA loaded nanoparticles. The injections were performed at day 0, 2, 4, 6, 8 in the caudal vein. Mice were sacrificed 24 h after the last injection. Tumours were conserved in TRIzol (Invitrogen, USA). RNA was extracted from tumours in TRIzol as indicated by the supplier. Resulting ARN samples were used to perform Reverse Transcription Quantitative Polymerase Chain Reaction (RT-qPCR), For total RNA extraction tumor samples were lyzed with 800 µL TRIzol. Chloroform (160 µL) was added, and the mixture was centrifugated at 13 000 rpm for 15 min. Then, 350 µL of the resulting aqueous phase were mixed with the same volume of isopropanol, incubated for 15 min at room temperature and centrifuged at 13 000 rpm for 15 min at 4°C. The pellet was washed twice using 70 % ethanol, let to dry and dissolved in 100 µL of water containing 0.5 unit/µL of RNasin ribonuclease inhibitor (Promega Corp., USA). Total RNA was quantified by measuring the optical density at 260nm using the ND-1000 spectrophotometer (Nanodrop, USA). Reverse transcription was performed on 1 µg of total RNA by adding 2 µL of Random Hexamers at 50 µg/µL (Promega), and heated at 65 ° C during 5 min. Then RNA was incubated with 0.5 µL of M-MLV Reverse Transcriptase (Promega) 200 unit/µL, 0.5 µL of dNTP 20 mM, 0.5 µL of RNasin 40 unit/µL and 4 µL of M-MLV RT 5X reaction buffer (Promega) for 1 h at 42°C.

Quantitative PCR (qPCR) was performed using SYBR GreenER qPCR SuperMix (Invitrogen) using 5 µL of cDNA diluted to 1/20 (v/v) in 25 µL final volume. Samples were amplified with 45 cycles using 7900HT Fast Real-Time PCR System (Applied Biosystems, USA) as follows: 2 min incubation at 50°C, 10 min at 95 ° C, followed by 45 cycles at 95°C over 15 s and 60°C over 1 min. The results are expressed in percentage compared to untreated tumor samples.

1.4. General in vivo tolerance of the nanoparticles

Mice were weighted every day during the experiment to check for toxicity. Immediately before sacrifice blood was collected from mice for further analysis by intracardiac punction under isoflurane anaesthesia. Blood was used for complete blood count, Aspartate amino transferase (AST)/Alanine Amino transferase (ALT) measurement and urea/creatinin measurement. AST/ALT are commonly used to monitor liver function while urea and creatinin are commonly used to monitor kidney fonction.

2. Results

2.1. Preparation of the immunonanoparticles

The preparation of the immunonanoparticles was performed in 3 steps according to the method proposed by Segura-Sanchez *et al.* [Segura-Sanchez et al., 2010]. At first, a biotinylated spacer was grafted on the nanoparticle corona. Another biotinylated spacer was coupled on the previously oxidized primary alcohol functions on the Fc fragment of an anti-cd99 antibody. The biotinylated antibodies and the biotinylated nanoparticles were assembled using neutravidin to form the immunonanoparticles directed against the cd99 surface glycoprotein expressed at the surface of the

targeted cells. The assembly was formed thanks to the strong affinity of biotin for avidin which has been known for a long time [Wright et al., 1947].

2.1.1. Biotinylation of the nanoparticle

The EZ-Link® Sulfo-NHS-LC-Biotin (A in table 1) did not allow to link biotin motives to the surface of the nanoparticles. In contrast, EZ-Link® TFP-PEO_3-biotin (B in table 1) allowed an efficient attachment of the biotin onto the surface of the nanoparticles (Table1). At a concentration of 1,4 mM, this spacer allowed to link up to 43 biotins per nanoparticle with a final concentration of biotin up to 1,53 10^{-6} mM/mL at a concentration in nanoparticles of 10 mg/mL. The grafting was confirmed by TEM with gold labeled avidine molecules as a revelation agent. No labeling could be seen on particles grafted with the EZ-Link® Sulfo-NHS-LC-Biotin (Figure 1 images 1 and 2). In contrast, with EZ-Link® TFP-PEO_3-biotin (Figure 1 images 3 and 4), TEM showed black dots at the surface the biotinylated nanoparticles corresponding to the gold avidin linked to the biotin motives.

Table 1: Biotinylation of PIBCA/MethylMethaAcrylate Rhodamine nanoparticles using two different biotinylated spacers: A: EZ-Link® Sulfo-NHS-LC-Biotin and B: EZ-Link® TFP-PEO_3-biotin.

N°	MM of chitosan in the corona (kDa)	Lutrol F68 (%)	Biotin spacer	Biotin spacer Initial concentration (mmol/mL)	Remaining biotine (mmol/mL)	Number of biotin by NP
1	70	2	A	0.7	0	0
2	70	2	A	1.4	0	0
3	70	2	B	0.7	$4.68\ 10^{-7}$	7
4	70	2	B	1.4	$1.78\ 10^{-6}$	25
5	20	3.5	B	1.4	$1.53\ 10^{-6}$	43

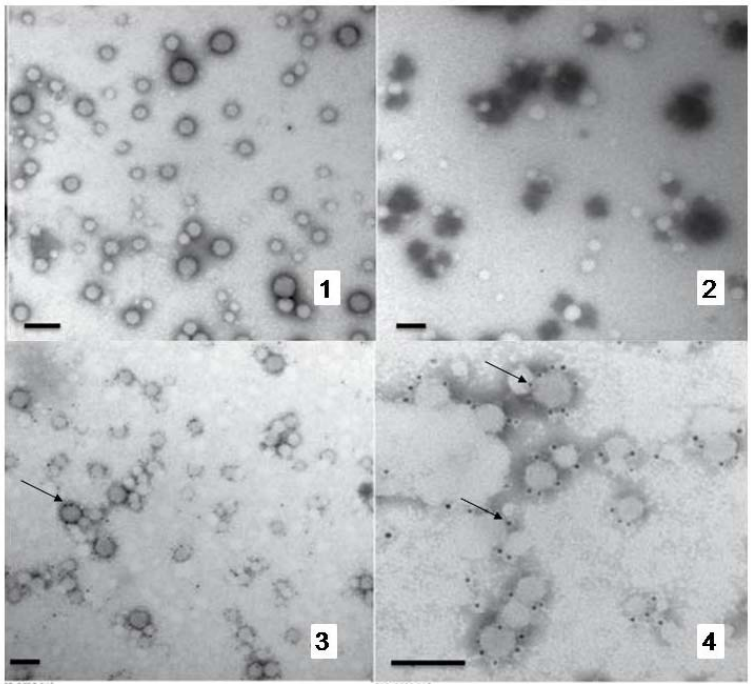

Figure 1: Transmission Electron Microscopy of nanoparticles modified by grafting biotin on their surface with the EZ-Link® Sulfo-NHS-LC-Biotin (Samples N° 1 and 2 in table 1) and the EZ-Link® TFP-PEO_3-biotin (Samples N° 3 and 4 in table 1) reagents. The presence of biotin residues on the nanoparticles surface was revealed using gold-Avidin. Scale bar = 100nm.

2.1.2. Biotinylation of the anti-cd99 antibody

Figure 2 shows flow cytometry analysis of untreated A673 cells (Figure 2A), A673 cells incubated with control biotinylated antibody (Figure 2B) and anti-cd99 biotinylated antibody (Figure 2C) revealed using FITC-avidin. There were no detectable fluorescent cells for untreated cells or cells treated with the control biotinylated antibody. However, cells treated with anti-cd99 biotinylated antibody demonstrated a green fluorescence peak. This demonstrated that anti-cd99 antibodies were biotinylated and that the biotin motive was still accessible for complexation with avidin. Moreover, this also showed that the biotinylation did not affect the ability of the anti-cd99 antibodies to bind their glycoprotein target on cell membranes.

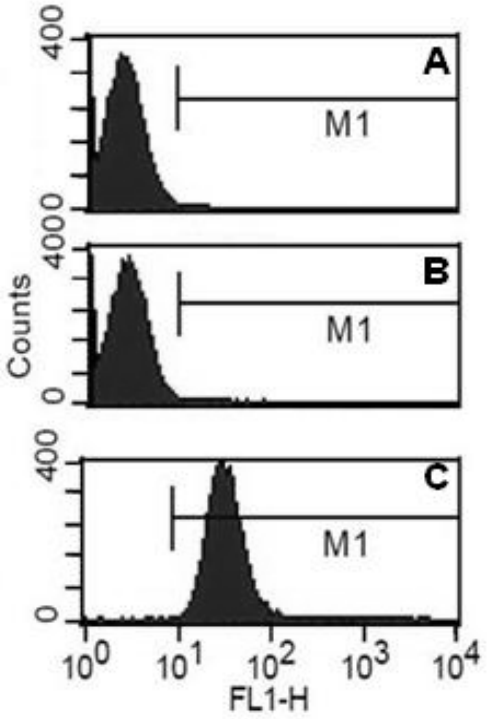

Figure 2: Flow cytometry analysis performed on A673 cells to evaluate the binding capacity and specificity of the anti-cd99 antibody to their targeted cells after biotinylation. Revelation of the antibody binding to the A763 cells was achieved using a fluorescein labeled streptavidin. Flow charts from A: Untreated cells; B: cells incubated with biotinylated control antibody; C: cells incubated with biotinylated anti-cd99 antibody.

2.1.3. Evaluation of the coupling efficiency of the biotinylated antibody and of the PIBCA/chitosan nanoparticles

Targeted nanoparticles were formed by the assembly of biotynylated anti-cd99 antibody with biotynylated nanoparticles using avidin thanks to the formation of biotin-avidin complexes. The ability of the biotin-avidin complex to efficiently bind antibodies on the surface of nanoparticles was verified using bicinchroninic acid (BCA) dosage, a colorimetric method used to measure protein concentration, and western blotting, a method used to reveal the presence of specific proteins in a sample.

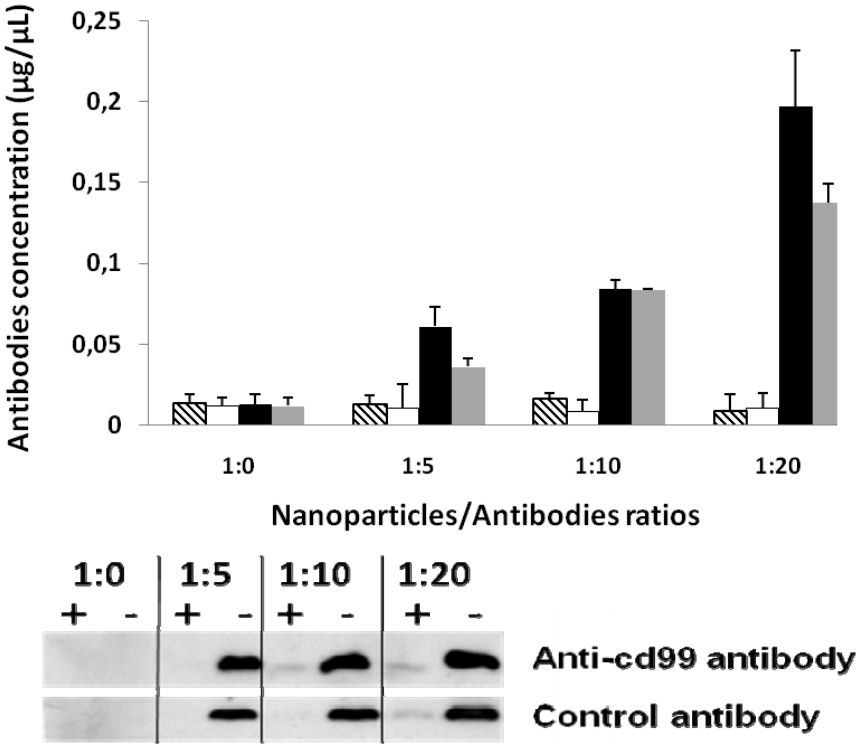

Figure 3: BCA dosage (top) and western blot analysis (bottom) of the remaining free antibodies found in biotinylated nanoparticle dispersions after incubation with or without avidin at different ratios. Theoretical ratio of the number of nanoparticles over the number of antibody molecules were: 1:0, 1:5, 1:10, 1:20. Hashed bars: biotinylated nanoparticles + avidin + biotinylated anti-cd99 antibody, white bars: biotinylated nanoparticles + avidin + biotinylated control antibody, black bars: biotinylated nanoparticles + biotinylated anti-cd99 antibody, grey bars: biotinylated nanoparticles + biotinylated control antibody

As shown in figures 3, there were no remaining free antibodies when the nanoparticles were incubated in the presence of avidin. On the contrary, without avidin, we showed that remaining free antibodies were detected. Moreover, the amount of free antibodies detected in the nanoparticle dispersion corresponded to the initial quantity of antibodies used to prepare the nanoparticles. This indicated that there was no non-specific binding of the antibodies on the cationic shell of the nanoparticles and that antibodies associated with the nanoparticles were only those coupled via the biotin-avidin grafted method used in the coupling procedure. Addition of avidin in media containing both the biotinylated antibody and the biotinylated nanoparticles allowed the formation of the immunonanoparticles.

2.2. Characterization of the nanoparticles

2.2.1. Size

The mean size of the nanoparticles was not significantly modified after biotinylation and after grafting of the antibodies, no matter the amount of antibody added at the surface of the nanoparticles (table 2). These results indicated that the size of the nanoparticles remained stable after biotinylation and after association of the antibody to form the immunonanoparticles.

Table 2: Size of the nanoparticles and complement activation triggered by the various types of PIBCA/Chitosan nanoparticles considered in this work (n = 3). Ab: anti-cd99 antibodies. Theorical ratio number of nanoparticles/antibody molecules: 1:5, 1:10, 1:20: siRNA:small interfering RNA ratio, PIBCA/MMA-Rh/Chitosan: rhodamine-labelled nanoparticles.

	Mean size ± SD (nm)	CAF ± SD (%)
PIBCA/Chitosan	66 ± 3	20 ± 9
PIBCA/MMA-Rh/Chitosan, siRNA (ratio 50)	-	14 ± 2
PIBCA/MMA-Rh/Chitosan	80 ± 2	17 ± 5
Biotinylated PIBCA/MMA-Rh/Chitosan	82 ± 4	14 ± 4
PIBCA/MMA-Rh/Chitosan:Ab, 1:5	82 ± 4	24 ± 2
PIBCA/MMA-Rh/Chitosan :Ab, 1:10	84 ± 3	25 ± 3
PIBCA/MMA-Rh/Chitosan :Ab, 1:20	85 ± 4	22 ± 4
Negative control (VBS^{2+})	-	13 ± 5
Positive control	-	91 ± 12

2.2.2. Morphology

Transmission electron microscopy (TEM) showed no differences in distribution, shape or size between PIBCA/MMA-Rhodamine nanoparticles and any of the PIBCA/MMA-Rhodamine nanoparticles grafted with various amounts of avidin/antibody complexes (Figure 4). However, immunonanoparticles with a number of grafting antibody molecules above 5 seemed to form aggregates during preparation of samples for TEM observation.

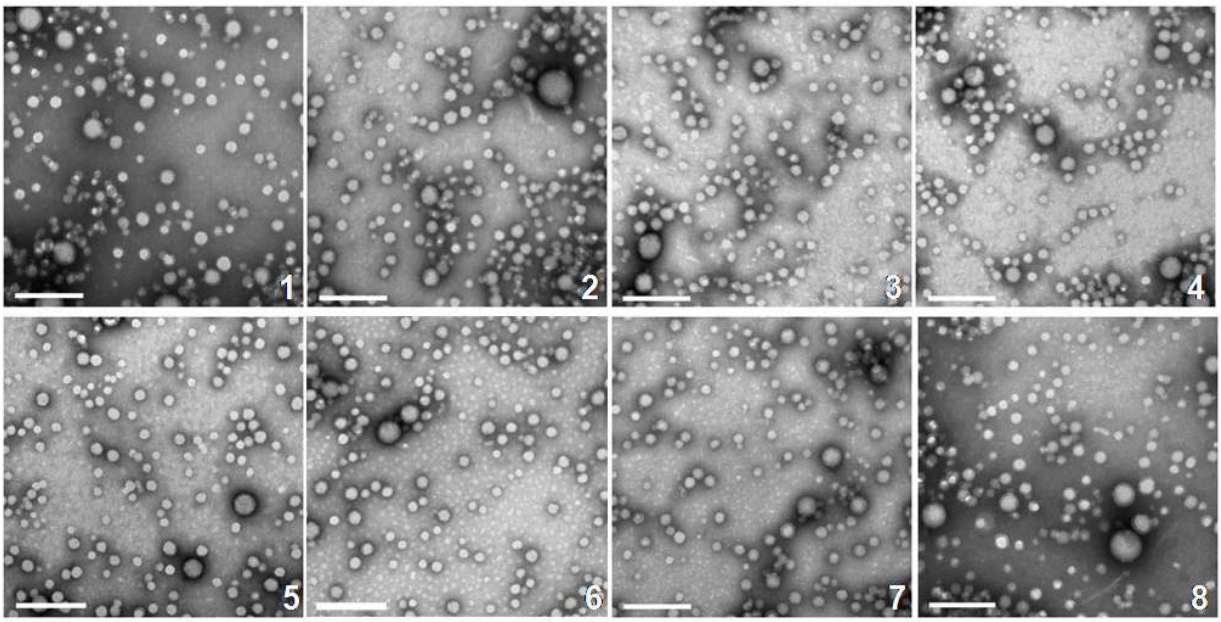

Figure 4: Transmission Electron Microscopy of targeted nanoparticles. Top line: NP carrying cd99 antibody, bottom line: NP carrying control antibody. Theorical ratio number of nanoparticles over the number of antibody molecules were: 1:0 (1,5), 1:5 (2,6), 1:10 (3,4), 1:20 (4,8). Scale bar: 200 nm

2.3. *In vitro* evaluation of the nanoparticles

2.3.1. Adsorption of siRNA onto nanoparticles

Capacity of biotinylated nanoparticles to adsorb siRNA was verified by performing adsorption experiments with a radiolabelled siRNA. Figure 5 shows that, in MilliQ® water, the maximum amount of siRNA adsorbed on the biotinylated nanoparticles was decreased by 13.6 % at a nanoparticles/siRNA mass ratio of 50, compared with the non-biotinylated nanoparticles. The decrease was equal to 9.5 % at a nanoparticles/siRNA mass ratio of 300. This was correlated with the decrease of the zeta potential comparing that of the non modified nanoparticles (+32±3 mV) with that of the biotinylated nanoparticles (+24±3 mV).

In saline medium, the difference between biotinylated and non-biotinylated nanoparticles was not significantly different at a Nanoparticles/siRNA mass ratio of 50, which was the ratio used for further *in vitro* and *in vivo* experiments.

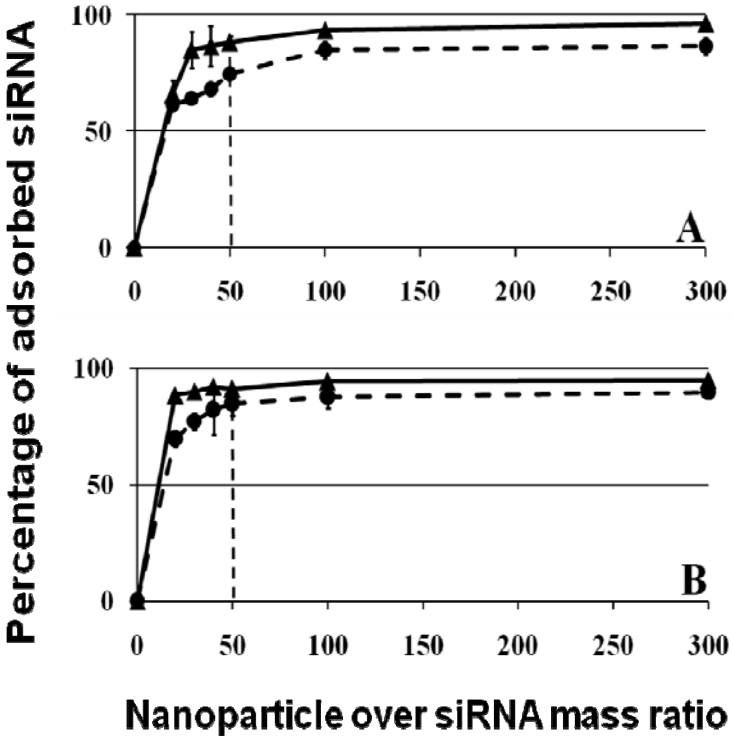

Figure 5: Adsorption of siRNA on nanoparticles. in MilliQ® water (A) and in HEPES/NaCl (B). Non modified nanoparticles (full triangles) and biotinylated nanoparticles (full circles).

2.3.2. Activation of the complement system

Results from the evaluation of the capacity of the nanoparticles to activate the complement system showed that none of the tested nanoparticles led to a complete activation (Table 2). Complement activation factors (CAF) measured for the nanoparticles ranged from 14±4 % to 23±3 % while a positive control of activating nanoparticles showed a CAF of 91±12 % and the spontaneous activation measured in the experimental conditions showed a CAF of 13±5 %. This indicated that the nanoparticles considered in this work were almost not activating regarding the complement cascade

even after modification of their surface by adding biotin, the antibody and the siRNA or by labelling the core of the nanoparticles with a fluorescent molecule.

2.3.3. Evaluation of the cytotoxicity of nanoparticles

The average 50 % growth Inhibitory Concentration (IC_{50}) of the nanoparticles after 24 h of contact in with A673 cells was evaluated. The PIBCA/ Chitosan nanoparticles showed an IC_{50} of 32 ± 3 µg/mL. The tolerance of the nanoparticles by cells was decreased when the core was labelled using MethylMetaAcrylate Rhodamine as the IC_{50} dropped to 18 ± 2 µg/mL. However, the grafting of biotin and of the entire antibody-avidin complex did not decrease further the tolerance of the nanoparticles by the A673 cells. Values of the IC_{50} were 16 ± 2 µg/mL and 15 ± 1 µg/mL respectively. These values of the IC_{50} were comprised in the ranged of IC_{50} reported previously for various types of PIBCA nanoparticles (1 to 120 µg/mL) [Chauvierre, et al. 2007]. They agreed with those found for the dextran decorated PIBCA nanoparticles (20 µg/mL) which were prepared by the same method than that considered in the present study.

2.3.4. Evaluation of the Cd99 expression on different Ewing sarcoma cell lines

Figure 6 shows flow cytometry analysis of various cell lines obtained after labeling cells with anti-cd99 antibody or with a control antibody. A673 (A), TC71 (B) and cd99 expressing Jurkat (C) cells show a shift of the fluorescence mean after incubation with the anti-cd99 antibody. On the contrary, cells which do not express cd99 (D) did not give any shift of the fluorescence mean. This indicated that Ewing's sarcoma cells lines A673 and TC71 were expressing the cd99 glycoprotein antigen. They can be used in the evaluation of a drug targeting strategy including the cd99 glycoprotein as the target.

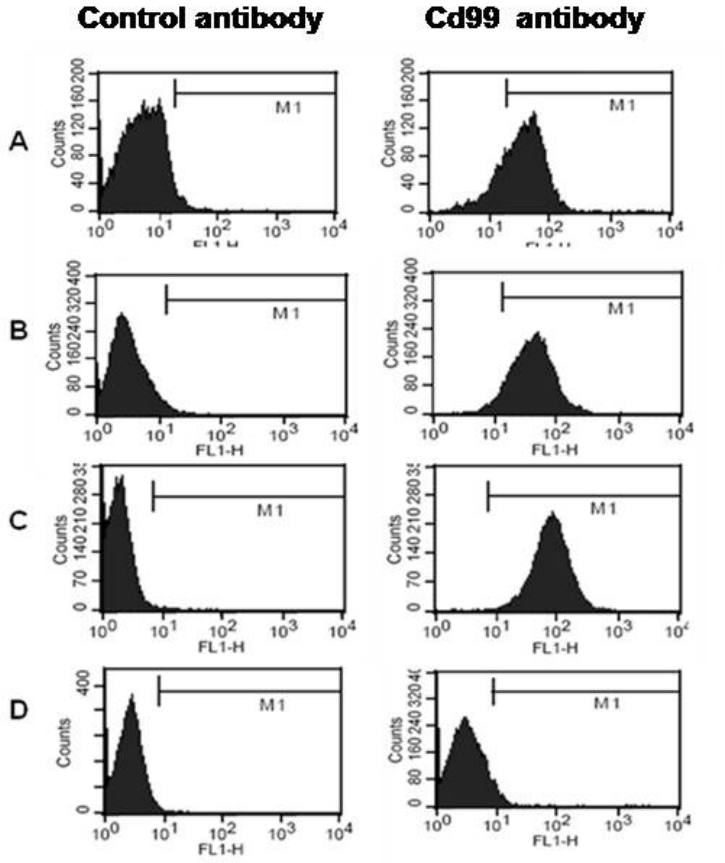

Figure 6: Evaluation of the cd99 expression on various cell lines. A: A673 cells, B: TC71 cells, C: cd99 positive Jurkat cells, D: cd99 negative Jurkat cells. Cells were first incubated with either a control antibody (left column) or the anti-cd99 antibody (right column) and revealed using an FITC coupled secondary antibody.

2.3.5. Confocal microscopy analysis

Confocal microscopy images of A673 Ewing's Sarcoma cell line treated with nanoparticles grafted with cd99 antibody or control antibody show that only nanoparticles carrying five units of the cd99 antibodies by nanoparticle could efficiently bind the cell membrane with high specificity of the recognition (Figure 7). It is noteworthy that A673 cells could be recognized by nanoparticles bearing a rather low amount of anti-cd99 antibody molecules on the surface. Indeed, only 5 molecules of the specific antibody were sufficient to achieve this recognition.

The recognition of cd99 by the targeted nanoparticles was shown by the red labeling of the cell membrane, due to the rhodamine core of the nanoparticles. To localize cell positions on the slide, the nucleus was stained with DAPI which appeared as a blue fluorescence.

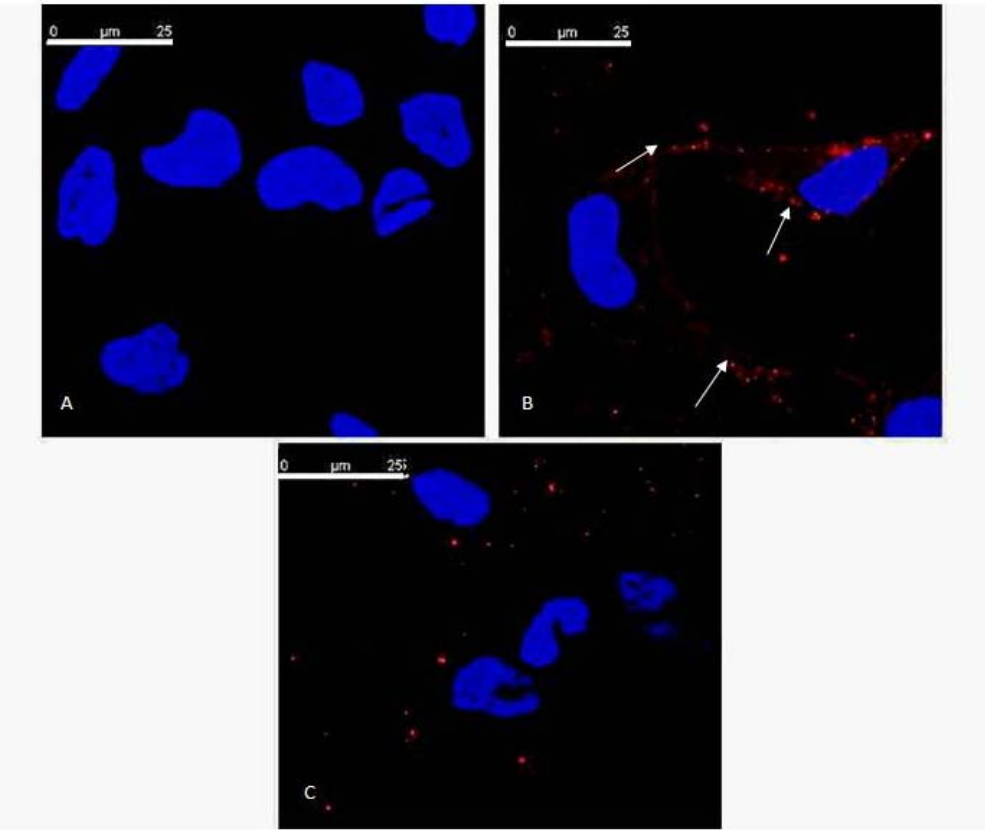

Figure 7: Confocal micrographs of cd99 expressing A673 cells untreated (A), treated with cd99 targeted nanoparticles (ratio 1:5) (B) and treated with the non modified nanoparticles used as control nanoparticles (ratio 1:5) (C) The nanoparticles (red fluorescence shown by the white arrows) were labeled in the core with a rhodamine containing fluorescent probe. Cells nucleus were stained with Dapi (blue fluorescence). Scale bars: 25 µm.

2.4. *In vivo* evaluation of the nanoparticles

2.4.1. *In vivo* efficiency of the nanoparticles to target siRNA against Ewing's sarcoma tumors xenografted in mice

Expression of EWS/Fli-1 was evaluated by qRT-PCR after injection of different formulations and control samples in nude mice (Figure 8).

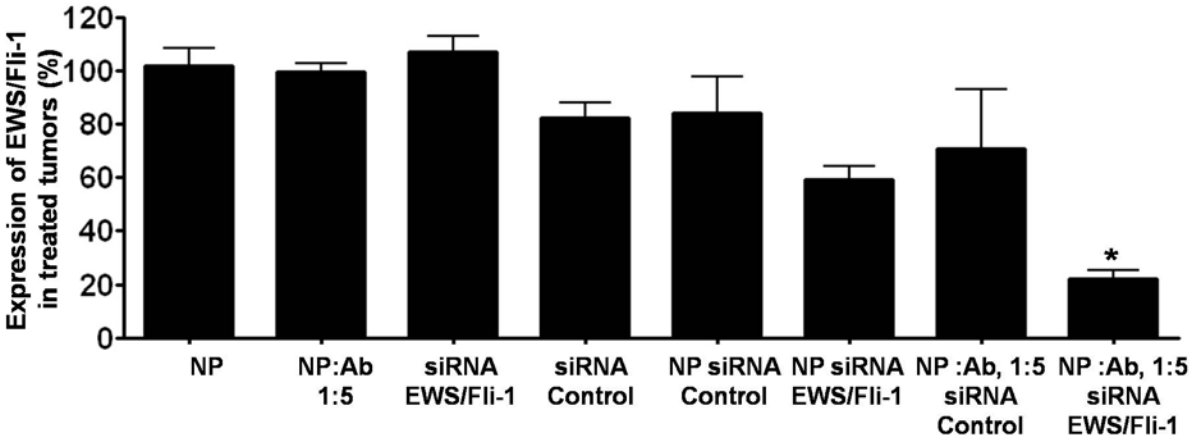

*Figure 8: Evaluation of the in vivo efficiency of the siRNA loaded nanoparticles. The expression of EWS/Fli 1 gene was measured by RT-qPCR. Results were expressed as a percentage of the mean level of expression found in control tumors 5NP, NP:AB 1:5, siRNA EWS/Fli-1, siRNA control). NP: Nanoparticles; Ab: cd99 Antibody. Statistics: * p<0.05, Kruskal-Wallis test.*

All experiments with siRNA described in figure 8 were made with the same amount of siRNA. The level of expression of the EWS/Fli-1 gene was compared with that found in mice treated with controls. The non-targeted nanoparticles carrying the siRNA showed an inhibition of 41 ± 9 % of the expression of the target gene after IV injection of a dose of 24 µg siRNA/kg/injection. Using the same dose of siRNA, the cd99 targeted nanoparticles inhibited the expression of EWS/Fli-1 at a much higher level 78 ± 6 %. All control experiments including mice treated with siRNA alone or with nanoparticles alone or with nanoparticles carrying control siRNA did not show any inhibition of the expression of EWS/Fli-1. Despite the highlight of a clear inhibition of the level of the expression of the oncogene in mice treated with the siRNA associated with targeted and untargeted nanoparticles, no inhibition of the growth of the tumors could be measured. These observations were provided considering a dosage of siRNA of 24 µg siRNA/kg/injection. It is noteworthy that a significant difference in tumor growth was observed after 24 days between untreated (relative tumor volume of 12 ± 4, n=11) and treated animals (relative tumor volume of 9 ± 2, n=4) ($p<0.005$, Mann & Whitney) by intravenous injection of a much higher dose of siRNA associated with untargeted nanoparticles (0.5 mg siRNA/kg/injection). At this higher dosage, the inhibition of the expression level of EWS/Fli-1 in tumors treated with untargeted nanoparticles carrying siRNA directed against EWS/Fli-1 was 71.2 ± 1.3 % after 9 days compared to tumors injected with a saline solution.

2.4.2. *In vivo* toxicity of the nanoparticles

The weight of the mice was monitored during all the experiment to detect possible toxicities, but no loss of weight was reported. The mean weight of the mice was 30g± 1g at the beginning of the study and 29g±2g at the end of the treatment. The Table 3 summarizes results of the tolerance study of the treatments. Blood parameters were not affected by treatments as indicated by no significant difference between the control group and the different treated groups neither in cell counts nor in parameters related to the renal function (urea, creatinine) and to the liver function (AST, ALT) (Table 3).

Table 3: General in vivo tolerance of mice treatments. Evaluation of blood parameters. NP: Nanoparticles; Ab: anti-cd99 antibody; ALT: Alanine aminotransferase; AST: Aspartate aminotransferase

	NP	NP:Ab, 1:5	siRNA EWS/Fli-1	siRNA control	NP siRNA Control	NP siRNA EWS/Fli-1	NP:Ab,1:5 siRNA Control	NP:Ab,1:5 siRNA EWS/Fli-1
Immune cells (m/mm³)	5± 2	4± 2	4± 2	7± 2	3± 2	3± 1	3± 2	4± 1
Erythrocytes (m/mm³)	8± 1	7± 1	9.4± 0.6	8± 2	9.2± 0.7	7± 3	7.9± 0.6	7.5± 0.7
Mean Cell Volume (fl)	55± 2	55± 3	56± 1	56.0± 0.4	57± 1	56.1± 0.8	55.8± 0.6	56.6± 0.9
Hematocrite (%)	52± 3	41± 8	53± 5	58± 8	52± 4	35± 7	44± 3	42 ± 5
Platelets (m/mm³)	746± 549	779± 486	917± 547	687± 350	614± 213	667± 462	422± 242	653± 484
Urea (mM)	10± 2	9± 1	9± 1	8.1± 0.3	10± 2	9± 2	10.1± 0.6	8± 1
Creatinine (µM)	17± 3	18± 7	24± 8	28± 15	26± 8	26± 8	18± 6	26± 4
ALT (IU/L)	51± 10	53± 17	54± 8	49± 37	44± 3	51.5± 0.7	62± 1	53± 7
AST(IU/L)	869± 224	994± 127	942± 310	930± 139	924± 154	1158± 124	702± 52	687± 221

3. Discussion

siRNAs are promising candidates for cancer treatment, especially in diseases such as Ewing sarcoma which present a molecular abnormality allowing to target specifically the cancerous cells. However, these therapeutic molecules are fragile and rapidly degraded in the blood stream. Moreover, they cannot pass biological barriers, including cell membranes, due to their hydrophilic nature. That is the reason why many attempts are made to carry those molecules to the tumors to improve their efficacy. Here we chose to use biocompatible polymeric nanocarriers that were previously used with success in thyroid papillary carcinoma with siRNA [de Martimprey et al., 2008, 2009]. In order to increase the targeting specificity of the nanoparticles and to decrease to dose required *in vivo*, we chose to address them by coupling an antibody directed against cd99. The antigen cd99, is well known. It is very often expressed in Ewing's sarcoma and is commonly used as a diagnosis marker

[Ambros et al., 1991, Dubois et al., 2010]. As shown in the present study, the cell lines A673 and TC71 expressed cd99 (Figure 6). So these cell lines were suitable to study nanoparticles targeted against Ewing's Sarcoma tumors.

In this study we showed an efficient biotinylation of the anti-cd99 antibody and an efficient biotinylation of the nanoparticle surface (Figure 3). Association between both the biotinylated antibodies and the biotinylated nanoparticles led to the formation of cd99 grafted immunonanoparticles thanks to the formation of biotin/avidin complexes. Transmission electron microscopy did not show any morphological difference between modified and unmodified nanoparticles indicating that the nanoparticles remained stable after surface modifications (Figure 4).

As the aim of this study was to design efficient and safe nanoparticles, we evaluated the ability of the nanoparticles to carry the siRNA directed against EWS/Fli-1 *in vivo.* Regarding association of siRNA with nanoparticles, no significant difference was observed between the adsorption of siRNA onto PIBCA/Chitosane nanoparticles and onto biotinylated PIBCA/Chitosane nanoparticles (Figure 5). Thus, the biotinylated nanoparticles were good candidates as nanocarriers for *in vivo* delivery of siRNA. Additionally, the toxicity of the nanoparticles was not influenced by both the biotinylation and the coupling of the surface antibodies. However, the nature of polymer composing the core seemed more critical as the introduction of a methylmethacrylate fluorescent marker decreased the IC_{50} on A673 cells in culture by almost 58% (Figure 8).

Despite the amounts of biotin, avidin and antibodies found on the nanoparticle surface, the surface modified nanoparticles did not activate the complement system which is part of the immune system of the host (Table 3). Therefore, they were expected to keep the stealth characteristics brought by the chitosane-pluronic corona.

In vitro, confocal microscopy analysis of A673 cells treated with cd99 targeted-Rhodamine-nanoparticles or with control-rhodamine-nanoparticle showed (Figure 7) a red labeling of the cell membrane with the targeted nanoparticles that can't be seen with untargeted-rhodamine-nanoparticles or control-rhodamine-nanoparticles. We evaluated the ability of a siRNA associated with the targeted immunonanoparticles to inhibit expression of EWS/Fli-1, which is considered to be the main genetic cause of Ewing's sarcoma [Delattre et al., 1992, Turc-Carel et al., 1984]. After retrieving treated tumors, RT- qPCR experiment was carried out. Results showed (Figure 8) a higher inhibition of the expression of EWS/Fli-1 in tumors when the siRNA was administered using the cd99-targeted immunonanoparticles, probably due to a larger amount of siRNA delivered to the tumor cells compared with untargeted nanoparticles. At 24 days after treatment with untargeted nanoparticles, there was a significant decrease of the tumor growth in treated tumors compared to untreated tumors. This was consistent with results previously obtained in vivo with other types of nanoparticles delivering antisense oligonucleotides on murine cells expressing the human oncogene EWS/Fli-1 [Elhamess et al., 2009]. The in vivo role of EWS/Fli-1 in the tumor growth is still badly documented. However, if EWS/Fli-1 would be validated as an oncogenic target, our results showed that it was possible to modulate its expression in conditions relevant to a therapeutic treatment (*i.e.* when the drug was administered once the tumor was already present). The fact that at 24 days, there was a significant decrease of the tumor growth in tumors treated with siRNA associated with nanoparticles compared to untreated tumors indicated that it was possible to obtain a human tumor

growth inhibition by modulation of the expression level of EWS/Fli-1 with a siRNA in A673 cells of human origin. Results reported here were consistent with those published earlier considering a model tumor formed from xenografted murine cells expressing the human EWS/Fli-1 [Elhamess et al., 2009]. In the perspective of the development of a treatment for human, the tumor model used in the present work was more relevant because it was composed of human cells originating from an Ewing's sarcoma.

To our knowledge only one other group has reported the use of targeted nanoparticles to deliver a siRNA directed against EWS/Fli-1 on human cell lines of Ewing Sarcoma [Hu-Lieskovan et al. 2005a]. Results have also showed that the carried targeted siRNA to the Ewing's sarcoma tumours led to an efficient reduction of the tumors growth. Hu-Lieskovan's study differed from our in various aspects. The cell line was different; the tumors were not subcutaneous xenografts hence the distribution and the efficacy of the particles may differ. Finally, the dose used was higher (50µg by injection for a 20g mouse, hence 2.5mg/kg/injection for a total of 6 injections, hence a total cumulative dose of 15mg/kg). In the present work, tumor inhibition, although modest, was observed with half of this dose (7mg/kg). However, it is noteworthy that the model used by Hu-Lisekovan *et al.* was probably more relevant and more difficult to treat than the subcutaneous model tumors used in our work. Moreover, as it is known that injection of high doses of siRNA may leed to non-specific off-target gene-silencing effect [Jackson et al., 2003] it is useful to demonstrate an effect, although modest, at a slightly lower dose. Additionally, Persengiev et al. have suggested that off-target gene-silencing could be a concentration-dependant related mechanism [Persengiev et al., 2004]. This could explain why growth inhibition was observed in our work at 7mg/kg whereas inhibition of the expression of the target gene EWS/Fli-1 was already clearly highlighted at a much lower dose (120µg/kg).

4. Conclusion:

In this work, we have developed biotinylated nanoparticles to be used as a new platform to design targeted polymeric immunonanoparticles with biotinylated ligands through a biotin-avidin coupling method. The approach was validated with targeted nanoparticles directed against cd99, well known as a diagnosis marker in Ewing's sarcomas. Those nanoparticles demonstrated their safety *in vitro* and *in vivo*. After intravenous injection siRNA carried by the targeted immunonanoparticles were able to inhibit the expression of the gene responsible of Ewing's sarcoma at a higher extent than untargeted nanoparticles in a model of subcutaneous implanted tumors. This demonstrated that the targeted immunonanoparticles were stealth *in vivo* in agreement with their low capacity to activate the complement system *in vitro*. Next step of this work will be to assess the efficacy of those nanoparticles against metastatic forms of Ewing's sarcoma as it is the metastasis development that are responsible for a bad prognosis factor in this cancer.

Acknowledgments:

The authors would like to thank the Association Leyla for founding AL Ramon's PhD grant. This work was supported by the InNaBioSanté foundation. The authors also thank Henkel Biomedical for kindly providing the IBCA.

References :

Alhaddad A, Adam MP, Botsoa J, Dantelle G, Perruchas S, Gacoin T, Mansuy C, Lavielle S, Malvy C, Treussart F, Bertrand JR. 2011. Nanodiamond as a vector for siRNA delivery to Ewing sarcoma cells. *Small* **7***:*3087-3095. DOI:10.1002/smll.201101193

Ambros IM, Ambros PF, Strehl S, Kovar H, Gadner H, Salzer-Kuntschik M. 1991. MIC2 is a specific marker for Ewing's sarcoma and peripheral primitive neuroectodermal tumors. Evidence for a common histogenesis of Ewing's sarcoma and peripheral primitive neuroectodermal tumors from MIC2 expression and specific chromosome aberration. *Cancer* **67***:*1886-1893. DOI: 10.1002/1097-0142(19910401)

Bertholon I, Lesieur S, Labarre D, Besnard M, Vauthie, C. 2006a. Characterization of dextran-poly(isobutylcyanoacrylate) copolymers obtained by redox radical and anionic emulsion polymerization. *Macromolecules* **39***:*3559-3567. DOI: 10.1021/ma060338z.

Bertholon I, Vauthier C, Labarre D. 2006b. Complement activation by core-shell poly(isobutylcyanoacrylate)-polysaccharide nanoparticles: influences of surface morphology, length, and type of polysaccharide. *Pharm Res* **23***:*1313-1323.DOI: 10.1007/s11095-006-0069-0.

Bravo-Osuna I, Ponchel G, Vauthier C. 2007. Tuning of shell and core characteristics of chitosan-decorated acrylic nanoparticles. *Eur J Pharm Sci* **30***:*143-154. DOI: 10.1016/j.ejps.2006.10.007

Chauvierre C, Leclerc L, Labarre D, Appel M, Marden MC, Couvreur P, Vauthier C. 2007. Enhancing the tolerance of poly(isobutylcyanoacrylate) nanoparticles with a modular surface design. *Int J Pharm* **338***:*327-332. DOI: 10.1016/j.ijpharm.2007.01.034

Daka A, Peer D. 2012. RNAi-based nanomedicines for targeted personalized therapy. *Adv Drug Deliv Rev*. DOI: 10.1016/j.addr.2012.08.014

de Martimprey H, Bertrand JR, Fusco A, Santoro M, Couvreur P, Vauthier C, Malvy C. 2008. siRNA nanoformulation against the ret/PTC1 junction oncogene is efficient in an in vivo model of papillary thyroid carcinoma. *Nucleic Acids Res* **36***:*e2. DOI: 10.1093/nar/gkm1094.

de Martimprey H, Bertrand JR, Malv, C, Couvreur P, Vauthier C. 2009. New core-shell nanoparticules for the intravenous delivery of siRNA to experimental thyroid papillary carcinoma. *Pharm Res* **27***:*498-509. DOI: 10.1007/s11095-009-0043-8.

Delattre O, Zucman J, Plougastel B, Desmaze C, Melot T, Pete, M, Kovar H, Jouber, I, de Jon, P, Rouleau G, Aurias A., Thomas G. 1992. Gene fusion with an ETS DNA-binding domain caused by chromosome translocation in human tumours. *Nature* **359***:*162-165.DOI: 10.1038/359162a0

Dubois SG, Epling CL, Teague J, Matthay KK, Sinclair E. 2010. Flow cytometric detection of Ewing sarcoma cells in peripheral blood and bone marrow. *Pediatr Blood Cancer* **54***:*13-18.DOI: 10.1002/pbc.22245

Elhamess H, Bertrand JR, Maccario J, Maksimenko A, Malvy C. 2009. Antitumor vectorized oligonucleotides in a model of ewing sarcoma: unexpected role of nanoparticles. *Oligonucleotides* **19***:*255-264. DOI: 10.1089/oli.2009.0197

Esiashvili N, Goodman M, Marcus RB Jr. 2008. Changes in incidence and survival of Ewing sarcoma patients over the past 3 decades: Surveillance Epidemiology and End Results data. *J Pediatr Hematol Oncol* **30***:*425-430. DOI: 10.1097/MPH.0b013e31816e22f3

Hu-Lieskovan S, Zhang J, Wu L, Shimada H, Schofield DE, Triche TJ. 2005a. EWS-FLI1 fusion protein up-regulates critical genes in neural crest development and is responsible for the observed phenotype of Ewing's family of tumors. *Cancer Res* **65***:*4633-4644. DOI: 10.1158/0008-5472.CAN-04-2857

Hu-Lieskovan S, Heidel JD, Bartlett DW, Davis ME, Triche TJ. 2005b. Sequence-specific knockdown of EWS-FLI1 by targeted, nonviral delivery of small interfering RNA inhibits tumor growth in a murine model of metastatic Ewing's sarcoma. *Cancer Res* **65***:*8984-8992. DOI: 10.1158/0008-5472.CAN-05-0565

Jackson AL, Bartz SR, Schelter J, Kobayashi SV, Burchard J, Mao M, Li B, Cavet G, Linsley PS. 2003. Expression profiling reveals off-target gene regulation by RNAi. *Nat Biotechnol* **21***:*635-637. DOI: 10.1038/nbt831.

Lin RY, Dayananda K, Chen TJ, Chen CY, Liu GC, Lin KL, Wang YM. 2012. Targeted RGD nanoparticles for highly sensitive in vivo integrin receptor imaging. *Contrast Media Mol Imaging* **7***:*7-18. DOI: 10.1002/cmmi.457

Liu P, Wang H, Wang Q, Sun Y, Shen M, Zhu M, Wan Z, Duan Y. 2012. cRGD conjugated mPEG-PLGA-PLL nanoparticles for SGC-7901 gastric cancer cells-targeted Delivery of fluorouracil. *J Nanosci Nanotechnol* **12***:*4467-4471. DOI: 10.1166/jnn.2012.6213.

Lv PP, Ma YF, Yu R, Yue H, Ni DZ, Wei W, Ma GH. 2012. Targeted delivery of insoluble cargo (paclitaxel) by PEGylated chitosan nanoparticles grafted with Arg-Gly-Asp (RGD). *Mol Pharm* **9***:*1736-1747. DOI: 10.1021/mp300051h.

May WA, Arvand A, Thompson AD, Braun BS, Wright M, Denny, CT. 1997. EWS/FLI1-induced manic fringe renders NIH 3T3 cells tumorigenic. *Nat Genet* **17***:*495-497.10.1038/ng1297-495. DOI:10.1038/ng1297-495

Nobs, L, Buchegger, F, Gurny, R, Allemann, E (2006): Biodegradable nanoparticles for direct or two-step tumor immunotargeting. *Bioconjug Chem* **17***:*139-145. DOI: 10.1021/bc050137k.

Persengiev SP, Zhu X, Green MR. 2004. Nonspecific, concentration-dependent stimulation and repression of mammalian gene expression by small interfering RNAs (siRNAs). *RNA* **10***:*12-18. DOI: 10.1261/rna5160904.

Rorie CJ, Thomas VD, Chen P, Pierce HH, O'Bryan JP, Weissman BE. 2004. The Ews/Fli-1 fusion gene switches the differentiation program of neuroblastomas to Ewing sarcoma/peripheral primitive neuroectodermal tumors. *Cancer Res* **64***:*1266-1277. DOI: 10.1158/0008-5472.CAN-03-3274.

Saxena V, Naguib Y, Hussain MD. 2010. Folate receptor targeted 17-allylamino-17-demethoxygeldanamycin (17-AAG) loaded polymeric nanoparticles for breast cancer. *Colloids Surf B Biointerfaces* **94***:*274-280. DOI: 10.1016/j.colsurfb.2012.02.001.

Segura-Sanchez F, Montembault V, Fontaine L, Martinez-Barbosa ME, Bouchemal K, Ponchel G 2010. Synthesis and characterization of functionalized poly(gamma-benzyl-L-glutamate) derivates and corresponding nanoparticles preparation and characterization. *Int J Pharm* **387***:*244-252.DOI: 10.1016/j.ijpharm.2009.12.016.

Srinivasan C, Peer D, Shimaoka M. 2012. Integrin-targeted stabilized nanoparticles for an efficient delivery of siRNAs in vitro and in vivo. *Methods Mol Biol* **820***:*105-116. DOI: 10.1007/978-1-61779-439-1_7.

Takigami I, Ohno T, Kitade Y, Hara A, Nagano A, Kawai G, Saitou M, Matsuhashi A, Yamada K, Shimizu K. 2011. Synthetic siRNA targeting the breakpoint of EWS/Fli-1 inhibits growth of Ewing sarcoma xenografts in a mouse model. *Int J Cancer* **128***:*216-226. DOI: 10.1002/ijc.25564.

Toub N, Bertrand JR, Tamaddon A, Elhamess H, Hillaireau H, Maksimenko A, Maccario J, Malvy C, Fattal E, Couvreur P. 2006. Efficacy of siRNA nanocapsules targeted against the EWS-Fli1 oncogene in Ewing sarcoma. *Pharm Res* **23***:*892-900. DOI: 10.1007/s11095-006-9901-9.

Turc-Carel C, Philip I, Berger MP, Philip T, Lenoir GM. 1984. Chromosome study of Ewing's sarcoma (ES) cell lines. Consistency of a reciprocal translocation t(11;22)(q24;q12). *Cancer Genet Cytogenet* **12***:*1-19. DOI: 10.1016/0165-4608(84)90002-5.

Vauthier C, Persson B, Lindner P, Cabane B. 2011. Protein adsorption and complement activation for di-block copolymer nanoparticles. *Biomaterials* **32***:*1646-1656. DOI: 10.1016/j.biomaterials.2010.10.026.

Wang L, Su W, Liu Z, Zhou M, Chen S, Chen Y, Lu D, Liu Y, Fan Y, Zheng Y, Han Z, Kong D, Wu JC, Xiang R, Li Z. 2012. CD44 antibody-targeted liposomal nanoparticles for molecular imaging and therapy of hepatocellular carcinoma. *Biomaterials* **33***:*5107-5114. DOI: 10.1016/j.biomaterials.2012.03.067.

Wright LD, Skeggs HR, Cresson EL. 1947. Affinity of avidin for certain analogs of biotin. *Proc Soc Exp Biol Med* **64***:*150-153. DOI: 10.3181/00379727-64-15729